Original

Fain, X.; Grangeon, S.; Bahlmann, E.; Fritsche, J.; Obrist, D.; Dommergue, A.; Ferrari, C.P.; Cairns, W.; Ebinghaus, R.; Barbante, C.; Cescon, P.; Boutron, C.:

Diurnal production of gaseous mercury in the alpine snowpack before snowmelt

In: Journal of Geophysical Research (2007) AGU

DOI: 10.1029/2007JD008520

Diurnal production of gaseous mercury in the alpine snowpack before snowmelt

Xavier Faïn,[1] Sylvain Grangeon,[1] Enno Bahlmann,[1] Johannes Fritsche,[2] Daniel Obrist,[3] Aurélien Dommergue,[1,4] Christophe P. Ferrari,[1,4,8] Warren Cairns,[5] Ralf Ebinghaus,[6] Carlo Barbante,[5] Paolo Cescon,[5] and Claude Boutron[1,7,8]

Received 7 February 2007; revised 5 July 2007; accepted 10 August 2007; published 13 November 2007.

[1] In March 2005, an extensive mercury study was performed just before snowmelt at Col de Porte, an alpine site close to Grenoble, France. Total mercury concentration in the snowpack ranged from 80 ± 08 to 160 ± 15 ng l^{-1}, while reactive mercury was below detection limit (0.2 ng l^{-1}). We observed simultaneously a production of gaseous elemental mercury (GEM) in the top layer of the snowpack and an emission flux from the snow surface to the atmosphere. Both phenomena were well correlated with solar irradiation, indicating photo-induced reactions in the snow interstitial air (SIA). The mean daily flux of GEM from the snowpack was estimated at ~9 ng m^{-2} d^{-1}. No depletion of GEM concentrations was observed in the SIA, suggesting no occurrence of oxidation processes. The presence of liquid water in the snowpack clearly enhanced GEM production in the SIA. Laboratory flux chamber measurements enabled us to confirm that GEM production from this alpine snowpack was first driven by solar radiation (especially UVA and UVB radiation), and then by liquid water in the snowpack. Finally, a large GEM emission from the snow surface occurred during snowmelt, and we report total mercury concentrations in meltwater of about 72 ng l^{-1}.

Citation: Faïn, X., et al. (2007), Diurnal production of gaseous mercury in the alpine snowpack before snowmelt, *J. Geophys. Res.*, *112*, D21311, doi:10.1029/2007JD008520.

1. Introduction

1.1. Mercury Cycle in the Environment

[2] Mercury (Hg) is present in the environment in various chemical forms and can be emitted by both natural [*Pyle and Mather*, 2003] and anthropogenic [*Pacyna et al.*, 2001] sources. In the atmosphere, gaseous elemental mercury (Hg°, GEM) is the predominant form with a northern hemispheric background of 1.5–2.0 ng m^{-3} [*Slemr et al.*, 2003] and a lifetime of about 6–24 months [*Lamborg et al.*, 2002]. Oxidized species of Hg such as particulate mercury (PM) and reactive gaseous mercury (RGM) are found at lower concentrations (pg m^{-3}) in the atmosphere, except near combustion sources and except under special conditions in the Arctic during spring [*Schroeder and Munthe*, 1998]. The major anthropogenic sources of Hg to the atmosphere include emissions from fossil fuel combustion, waste incineration, chlor-alkali plants and metal smelting and processing [*Pacyna and Keeler*, 1995].

1.2. The Role of Snow Surfaces in Polar Areas

[3] Polar studies have shown that snow surfaces in the Arctic play an important role in the mercury cycle. High latitude snowpacks could act as a sink for GEM [*Ferrari et al.*, 2004a], and halogens are likely involved in homogenous and heterogeneous processes leading to GEM oxidation in the air of snow. Moreover, Atmospheric Mercury Depletion Events (AMDEs), which occur after polar sunrise in the atmosphere both in the Arctic [*Schroeder and Munthe*, 1998] and in Antarctica [*Ebinghaus et al.*, 2002] can lead in some cases to a fast deposition of oxidized forms of onto snow surfaces [*Lindberg et al.*, 2002]. As a result, the arctic seasonal snowpack is suspected to contribute to the contamination of the aquatic reservoir during snowmelt. The polar snowpack can also act a source of GEM to the atmosphere. Photodissociation of Hg(II) complexes [*Lalonde et al.*, 2003] was proposed to explain GEM emissions from snow surfaces.

1.3. The Role of Snow Surfaces in Temperate Areas

[4] Although polar areas have been intensively investigated for several years, few studies have investigated the

[1]Laboratoire de Glaciologie et Géophysique de l'Environnement (UMR 5183 CNRS/Université Joseph Fourier), St Martin d'Heres cedex, France.
[2]Institute of Environmental Geosciences, University of Basel, Basel, Switzerland.
[3]Desert Research Institute, Division of Atmospheric Sciences, Reno, Nevada, USA.
[4]Polytech' Grenoble, Université Joseph Fourier, Grenoble cedex, France.
[5]Environmental Sciences Department, University of Venice, Venice, Italy.
[6]Institute for Coastal Research, GKSS Research Centre, Geesthacht, Germany.
[7]Unité de Formation et de Recherche de Physique, Université Joseph Fourier, Grenoble cedex, France.
[8]Also at Institut Universitaire de France.

0148-0227/07/2007JD008520

role of snow surfaces in the midlatitudes. A recent study by *Blais et al.* [2005] has reported a contamination of the ecosystems in these areas with fish mercury levels exceeding health consumption guidelines established by the WHO in several Pyrénées lakes (450 to 2500 m a.s.l., France). In the Alps, *Ferrari et al.* [2002] measured both total Hg (Hg_T) and reactive Hg (Hg_R) concentrations in the seasonal snow cover. However, to fully understand the cycle of Hg in midlatitude areas, we must also investigate the dynamics of GEM. Additionally, the fate of Hg during snowmelt and the possible contamination of ecosystems are major issues in alpine regions with a high population density. Therefore we carried out a full study of GEM, Hg_T and Hg_R in an alpine snowpack at Col de Porte Meteo France Center (1326 m a.s.l.), close to Grenoble, France. The specific goals were to evaluate Hg_T and Hg_R in alpine snow, to investigate GEM dynamics in the alpine snowpack for the first time and to document fluxes between the alpine snowpack and the atmospheric surface layer using both field measurements and laboratory data.

2. Experimental Section

2.1. Site Description

[5] We conducted GEM monitoring and snow sampling from 9 March to 24 March 2005 at the CEN (Centre d'Etude de la Neige), a Meteo France research center dedicated to snow studies. CEN is located on the north face of the Col de Porte pass, in the Chartreuse mountains, French Alps (45, 29°N, 5, 77°E, 1326 m a.s.l.). Col de Porte is located 10 km north of Grenoble, close to a recreation area where about 50 cars can park on Saturday or Sunday. Thus this area could not be considered as a pristine location, due to road traffic and the proximity of a city with half million inhabitants. Meteorological parameters as well as snowpack characteristics were continuously recorded by Meteo France. Surface snow temperature was measured using an infrared sensor Testoterm with an uncertainty of 1°C. Solar irradiation was recorded using a pyranometer Kipp & Zonen CM14. Snowpack temperatures at 20, 40, 60, 80, 100, and 120 cm depth were measured with highly sensitive and calibrated temperature probes (Pt 100, Honeywell Control System) inserted in the Teflon® head of GEM snow probes (see below). Temperature uncertainty of Pt 100 was estimated at about 0.5°C.

2.2. Reactive and Total Mercury in Snow and Meltwater

[6] On March 16, Snow samples were collected at CEN each 20 cm from the surface down to the depth of 80 cm. Snow samples were stored in the dark at −20°C until analysis in April, 2005. On 19 March, we also collected three water samples from runoff receiving the melting snow close to the snow sampling location. These runoffs are fed by snowmelt and disappear at the end of spring when the snowpack has disappeared. However, these flows could be sufficient to flush away sediments or organic materials in their wake. Water samples were not filtered; they were acidified and analyzed immediately after sampling. For both snow and water sampling, we used ultra clean Teflon® bottles and clean sampling procedures [*Boutron*, 1990; *Ferrari et al.*, 2000]. We analyzed for Hg_R and Hg_T in snow, and for Hg_T in water samples. Hg_R corresponds to the fraction of mercury involved in easily reducible complexes by $SnCl_2$ or $NaBH_4$ such as $HgCl_2$, $Hg(OH)_2$, HgC_2O_4 [*Lindqvist and Rodhe*, 1985]. Total Hg includes Hg_R and stable complexes such as HgS, Hg^{2+} bound to sulfurs in humic compounds and some organomercuric species [*Lindqvist and Rodhe*, 1985]. We performed triplicates analysis for all measurements.

[7] Hg_R was determined at the Department of Environmental Science of the University Ca'Foscari of Venice (Italy), using an Agilent 7500i ICP-QMS (Agilent Technologies, Yokogawa Analytical Systems, Tokyo, Japan). Snow samples were melted just prior to analysis. After reduction with a 0.1% (w/v) $NaBH_4$ solution stabilized with a pellet (∼0.1 g) of NaOH, GEM was swept from the solution to plasma by an adapted gas liquid separator from a Perkin Elmer FIAS. Instrument calibrations were carried out with Hg standards prepared from serial dilutions of a monoelemental Hg solution at 1000 μg ml^{-1} (CPI International Santa Rosa, CA, USA). The detection limit of Hg was calculated as three times the standard deviation of the blank and was ∼0.2 ng l^{-1} for a 1 mL of sample.

[8] Total mercury measurements were carried out at LGIT (Grenoble, France) using an A.M.A. 254 (Advanced Mercury Analyser 254, Altec Ltd, Czech Republic). *Roos-Barraclough et al.* [2002] have described this apparatus and shown that the A.M.A. is fully compliant with E.P.A. standard method 7473 [*EPA*, 1998]. No digestion of the sample is required: the sample is heated (850°C) and combusted under a flow of oxygen. Even Hg trapped in mineral matrices is transferred to the gas phase. The mercury is then amalgamated on a gold trap, which is subsequently released in the elemental form and finally detected at 253.7 nm using atomic absorption spectrometry. A standard reference material (C.R.M. 7002, [Hg] = 0.090 ± 0.012 ppm) was used for the calibration of the apparatus and a recovery rate of ∼103% was achieved using six standard measurements. The detection limit, calculated as three times the standard deviation of the blank, was 0.04 ng of mercury.

2.3. GEM in the Air of Snow and in the Atmosphere

[9] Two gas phase mercury analysers (Model 2537A; Tekran Inc., Toronto, Canada) were used for the determination of GEM in ambient air, snow interstitial air (SIA) and for flux measurements using a dynamic chamber. The pre-filtered air stream (soda lime trap and 0.2 μm Teflon® particle filter) was collected on two gold cartridges A and B. GEM was thermally desorbed and detected by cold vapor atomic fluorescence spectrometry at 253.7 nm (Tekran, 1999). Dual gold cartridges allowed alternate sampling and desorption, resulting in continuous measurement of GEM on a predefined time base. The set-up, accuracy and precision of this instrument have been assessed during field intercomparisons at an urban/industrial site [*Schroeder et al.*, 1995] and at a remote marine background location. The Tekran analysers were operated with a 5-min sampling frequency and the air was sampled at a flow rate of 1.5 l min^{-1}. The analysers were calibrated every 25 h with an internal automatic permeation source injection. Additional manual injections were also carried out to ensure the reproducibility of the measurements. The detection limit for GEM in this operation mode is about

0.15 ng m^{-3}. From 10 to 14 March we sampled ambient air 150 cm above the snow surface. From 18 to 21 March, we used a 5-port Teflon® solenoid switch unit for measuring successively GEM concentration at 10 cm, 70 cm, 130 cm, 200 cm and 270 cm above the snow surface. This approach has been used to find out if a gradient of GEM concentrations could be detected indicating either deposition or emission processes above the surface as has been measured by *Obrist et al.* [2006] in a subalpine site. The concentration of GEM in SIA was intensively investigated from 9 to 10 March, March 15 to 17 from, and from 22 to 24 March. We used GAMAS probes (Gaseous Mercury in Interstitial Air in Snow) at several depths to measure GEM concentrations between 20 and 120 cm depth below the snow surface [*Dommergue et al.*, 2003a]. This system has been used successfully in different Arctic sites, for example, at Station Nord, Greenland [*Ferrari et al.*, 2004a], Kuujjuarapik, Canada [*Dommergue et al.*, 2003c] and Ny-Ålesund, Svalbard [*Ferrari et al.*, 2005]. Five GAMAS probes were connected to the Tekran analyser, using a 5-port Teflon® solenoid switch [*Fritsche et al.*, 2006]. This set-up allowed a cyclic sampling of each probe every 10 min. Measurements were performed in duplicates or triplicates. For triplicate sampling, mean uncertainty was ~0.94% independently of the depth investigated. Blanks of the probes were 0.05 ± 0.05 ng m^{-3}. Because liquid water entered the sampling lines when temperature in the snowpack rose about 0°C, we were not able to sample GEM in snow interstitial air during warm afternoons and nights.

2.4. Reliability of Interstitial Air Sampling

[10] Many compounds such as ozone [*Petersen et al.*, 2001], nitrogen oxides [*Honrath et al.*, 2002], formaldehyde [*Sumner and Shepson*, 1999], H_2O_2 [*Bales et al.*, 1995] and recently GEM [*Dommergue et al.*, 2002; *Steffen et al.*, 2002; *Ferrari et al.*, 2004a] have previously been measured in the air of snow. The transfer of chemicals in the air of snow and the exchanges with the atmosphere are driven mainly by two processes. First by diffusion which is a relatively slow transport process and the result of gradients in concentration and temperature, and second by ventilation which is caused by wind turbulence [*Albert and Shultz*, 2002]. Ventilation can significantly increase the rate of transfer of chemicals in the air of snow. Air pumping for analysis can generate a significant forced ventilation when the sampling flow rate is above 2 l min^{-1} [*Albert et al.*, 2002]. We were able to minimize this effect using a low flow rate at 1.5 l min^{-1}. Assuming that the 15 l of air sampled for each GEM measurement was originating from a sphere located at the vicinity of the probe, we estimated that the interstitial air was sampled in a radius of 10 cm around the probes. However, measurement at 20 cm depth could be confounded by cosampling of ambient air.

2.5. Flux Measurements

[11] GEM fluxes between the snowpack and the atmosphere were measured both in the field and laboratory using a flux chamber.

2.6. Field Measurements

[12] Snow-to-air fluxes were measured in 10 min intervals on the Col de Porte snowpack from March 18 to 25 using dynamic flux chambers similar to those used previously over soils [*Engle et al.*, 2001; *Obrist et al.*, 2005]. The flux chamber covered an area of 29 × 12 cm^2. The chamber was 10 cm high, and pushed 5 cm into the snow so that a headspace of 5 cm was above the snowpack. On one side, holes in the chamber wall enabled ambient air to enter the chamber (inlet) while on the other side we connected a Teflon® line for air pumping (outlet). A two-port switch unit (Tekran model 1110) connected to a Tekran 2537A analyzer controlled alternating sampling between two ¼" Teflon® lines. The first line was directly connected to the outlet of the chamber. The second line enabled sampling air at the inlet of the chamber. Particulate filters (0.2 μm) were mounted at the ends of both lines. The chamber was made of Polycast SOLACRYL™ SUVT, which is characterized by high transmissivity for UVB (~80% at a wavelength of 270 nm). Blanks were measured by sealing the bottom of the chamber with a Polycast SOLACRYL™ SUVT plastic plate and resulted in fluxes of 0.02 ± 0.11 ng m^{-2} h^{-1} for cartridge A and 0.03 ± 0.14 ng m^{-2} h^{-1} for cartridge B.

2.7. Laboratory Measurements

[13] We also conducted experiments using a laboratory flux chamber system and surface snow samples collected during the field campaign. We specifically assessed the influence of solar radiation, snow temperature and snowmelt on GEM emission processes. Snow samples were collected in the field using clean methods. Therefore the chemical composition at the time of collection should have been preserved. However, due to transportation, the cold storage of samples and the method used to introduce the snow into the laboratory flux chamber, the physical structure of the snow is partly lost. In this way surfaces that could play a role in the chemical reactivity of GEM may have been altered. A detailed description of the laboratory flux chamber is given by *Balhmann et al.* [2006]. This set-up can simulate snow-to-air exchange of gaseous compounds under controlled conditions of temperature and light radiation, and was used for preliminary studies by *Dommergue et al.* [2007]. Snow samples were placed in the Teflonized chamber, and ambient air which has been cleaned over active charcoal was pumped through the chamber at a predefined flow rate. Solar radiation was simulated by means of a short arc lamp (2000 W Xenon). The lamp was operated without any optical filter (wavelength below 280 nm), and with optical filters cut off at 295 nm and 340 nm. A cut off of 295 nm corresponds to the natural solar radiation under clear sky conditions. Total radiation intensity varied between 0 and 120 W m^{-2}. The flux chamber temperature was set to −4°C, except during the simulation of the snowmelt where we increased the temperature to +1°C.

2.8. Calculation

[14] GEM fluxes in the field and laboratory were calculated using the following equation:

$$F = \frac{C_O - C_I}{A} \times Q,$$

Table 1. Total Mercury Concentration in the Snowpack From the Surface to 80 cm Depth, Sampled at the End of the Field Campaign

Depth, cm	Hg_T, ng l^{-1}	Hg_R, ng l^{-1}
10	160 ± 15	<DL (0.2)
20	132 ± 13	<DL (0.2)
40	123 ± 13	<DL (0.2)
60	158 ± 16	<DL (0.2)
80	80 ± 08	<DL (0.2)

where F is the flux in ng m^{-2} h^{-1}, C_O and C_I are GEM concentrations in ng m^{-3} at the outlet and inlet ports respectively, A the surface area of the chamber in m^2 and Q the airflow rate in l min^{-1}. For the field flux chamber, A and Q were 348 cm^2 and 1.5 l min^{-1}. A and Q for the laboratory flux chamber were 0.2 m^2 and 5 l min^{-1} respectively.

3. Results

3.1. Snowpack Characteristics and Meteorological Conditions

[15] Heavy snowfall occurred on 6 March, and field measurements started on 7 March with a 130 cm thick snowpack. We had no more snow precipitation during the field campaign, and the thickness of the snowpack decreased progressively to 80 cm on 24 March. A pit was dug on 15 March for stratigraphy and density measurements. We observed a typical snowpack of isothermal metamorphism with melt events. Two icy layers (0.3–0.6 cm thick) were found at ~73 cm and ~81 cm depth. Warm days and clear nights led to the formation of a melt freeze crust on the top. Density increased progressively from ~0.2 g cm^{-3} at the snow surface to ~0.4 g cm^{-3} at the bottom of the snowpack. Four periods were identified to describe the variations of atmospheric and snow surface temperatures. From 7 to 10 March, snow surface and air temperatures stayed below zero, with no clear diurnal pattern. From 11 to 14 March, the snow surface was characterized by diel temperature pattern between −17°C and 0°C and atmospheric temperature stayed between −5°C and 2°C. From 15 to 21 March, the snow surface showed a daily variation pattern with a minimum around −4°C at night and a maximum at 0°C during the day. Atmospheric temperatures were above 0°C both at night and during the day with a maximum of about 15°C. Finally, on 22, 23, and 24 March during nights and days, surface snow temperatures were constant at 0°C, and atmospheric temperatures were always positive. During the whole field campaign, we observed low winds with a maximum speed of about 2 m s^{-1} on March 7. Irradiation showed a clear diel signal, but due to the location of CEN research center on the north face of the pass, and forest on its east side, direct solar radiation could not reach the snow surface before 9:30 in the morning.

3.2. Mercury Concentrations in Snow Pits and Meltwater

[16] Hg_R and Hg_T concentrations measured in the snowpack from the surface to 80 cm depth are reported in Table 1. Hg_R concentrations were always below the detection limit of the method (0.2 ng l^{-1}). Hg_T concentrations of 79 ± 1 ng l^{-1}, 63 ± 3 ng l^{-1} and 74 ± 2 ng l^{-1} were measured in the snowmelt runoff.

3.3. Variations of GEM Concentrations With Depth in the SIA

[17] Atmospheric GEM concentration during the field campaign was on average 1.8 ± 0.4 ng m^{-3} (n = 2300). From 18 to 22 March, no GEM gradient was observed between 10 and 200 cm above the surface. Figure 1 presents GEM profiles measured in the SIA on 15 March. We observed similar temporal variations of GEM concentration in the SIA during the whole field campaign. Figure 1 shows that all concentrations stayed permanently above atmospheric level from 6:30 to 14:00. Early in the morning, we measured relatively homogenous concentrations around 2.8 ng m^{-3} at all depths. From 6:00 (i.e., sunrise) to 13:00, we observed a strong increase in GEM concentration in the first centimeters of the snowpack. Before 10:00, highest concentrations were measured at 20 cm depth and we observed a decrease of GEM levels with depth. From 10:00 to 13:00, the highest concentrations were measured at 40 cm depth. Finally, maximum GEM concentrations of about 8 ng m^{-3} were measured at 40 cm depth around noon. Data obtained from the 20 cm depth probe have to be considered carefully because cosampling of atmospheric air is likely as mentioned before. Consequently, concentrations within the surface snowpack could be higher than the measured ones.

3.4. Variations of GEM Concentrations With Irradiation and Temperature in the SIA

[18] GEM concentrations measured during the entire field campaign in the snowpack at 20 and 80 cm depth are reported on Figure 2 with mean solar irradiation. GEM levels at 20 cm depth increased simultaneously with solar irradiation to reach concentrations as high as ~9 ng m^{-3}. Deeper in the snowpack, a delay was observed between increases of irradiation and GEM concentration. As shown in Figure 3, there was no clear trend in GEM variation with temperature below 0°C. However, as soon as temperature reached 0°C (i.e., snow was melting), we noticed a significant increase of GEM concentration in the SIA.

3.5. GEM Fluxes Between the Snowpack and the Atmosphere

[19] Figure 4 displays GEM exchange fluxes from the snowpack to the atmosphere from 18 to 20 March and from 22 to 24 March. GEM fluxes exhibited distinct diurnal patterns strongly correlated with solar irradiation. We observed peak emissions of GEM from the snowpack to the atmosphere during the day around 1.4 to 3.3 ng m^{-2} h^{-1} (see Table 2). Integration over the entire daytime period (from 6:00 to 21:00) resulted in daily GEM emissions of 3.9 to 12.2 ng m^{-2} d^{-1}. Over the entire measurement campaign of five days, this loss was estimated at ~50 ng m^{-2}. We measured mean incorporation fluxes of about ~0.15 ± 0.07 ng m^{-2} h^{-1}, from 21:00 to 6:00 during five days. Chamber blanks were determined at the beginning of the campaign and yielded a flux overestimation of 0.02 ± 0.11 ng m^{-2} h^{-1} (cartridge A) and 0.03 ± 0.14 ng m^{-2} h^{-1} (cartridge B). As deposition fluxes were close to the detection limit, we could not conclude that GEM incorpo-

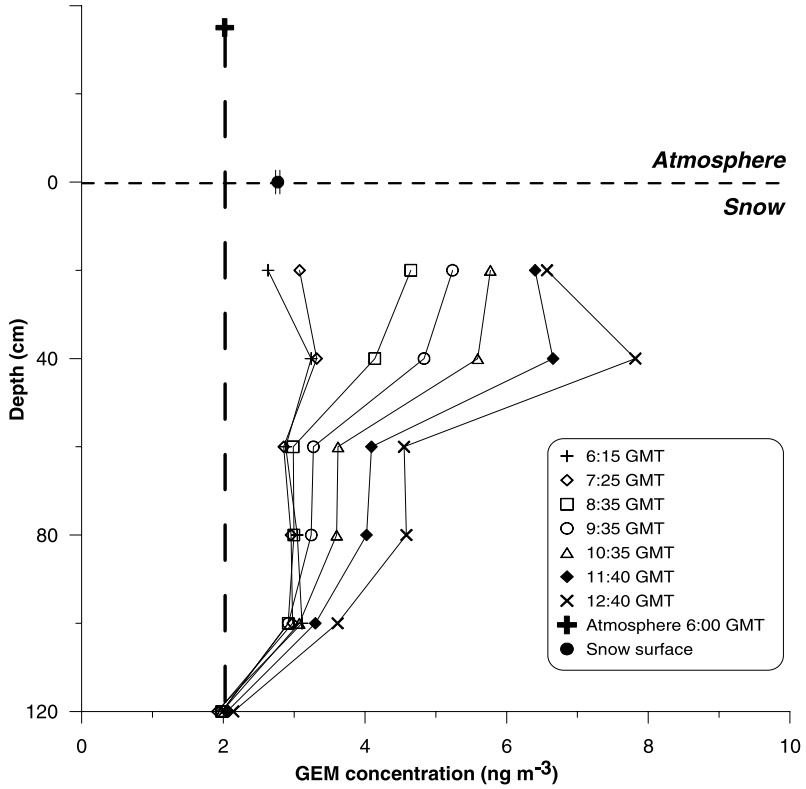

Figure 1. GEM profiles in interstitial snow air from the surface to 120 cm depth on March 15. Surface concentration reported here is an average of 20 measurements obtained the same day between 1:00 and 3:00 pm. The atmospheric level is the concentration determined at 6:00 am before sunrise. The error bar reported at the surface is one standard deviation of the mean values.

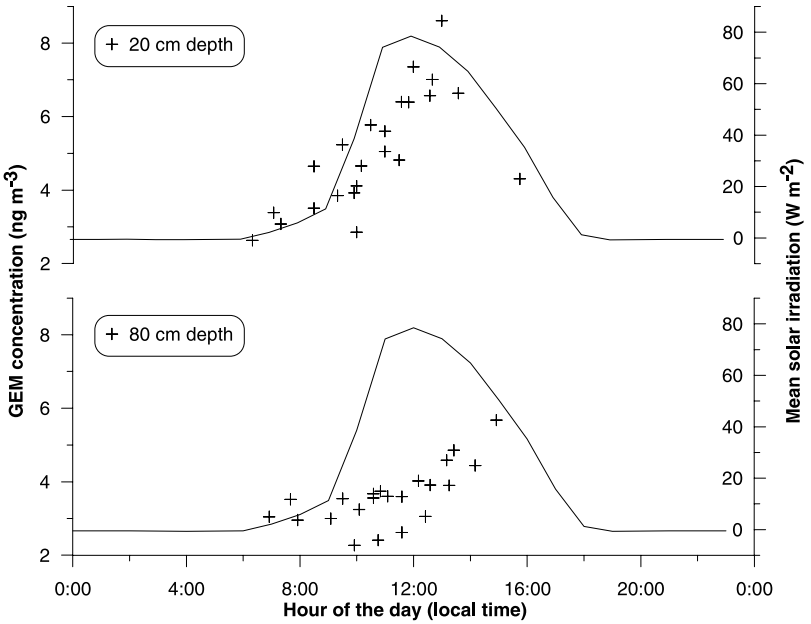

Figure 2. Variation of GEM concentrations in the snowpack (ng m^{-3}) at 20 and 80 cm depth with time. All data obtained during the field campaign are reported. Solar radiation is the mean calculated for the entire measurement period.

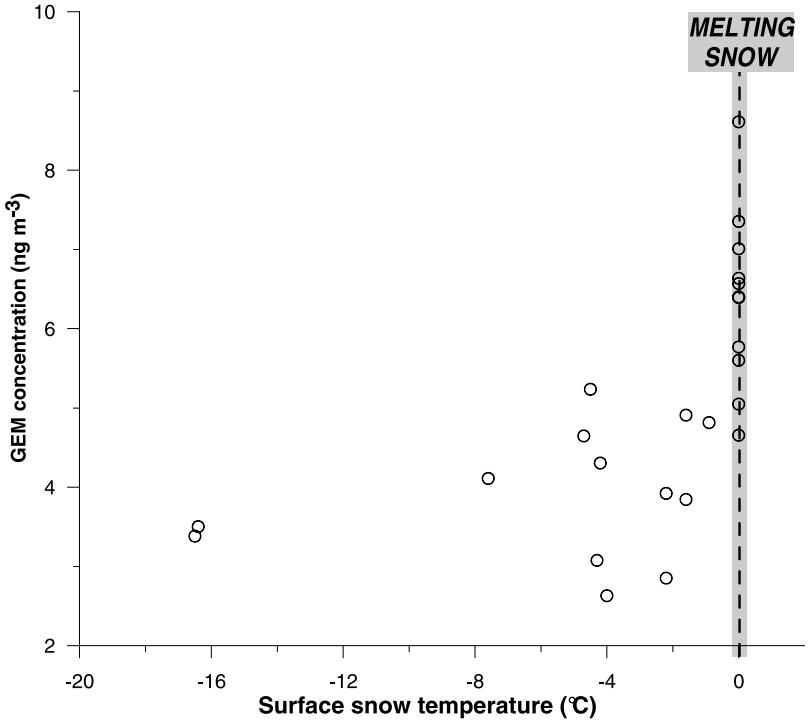

Figure 3. Increase of GEM concentration (ng m^{-3}) in the snow interstitial air at 20 cm depth with snow temperature from March 9 to 24.

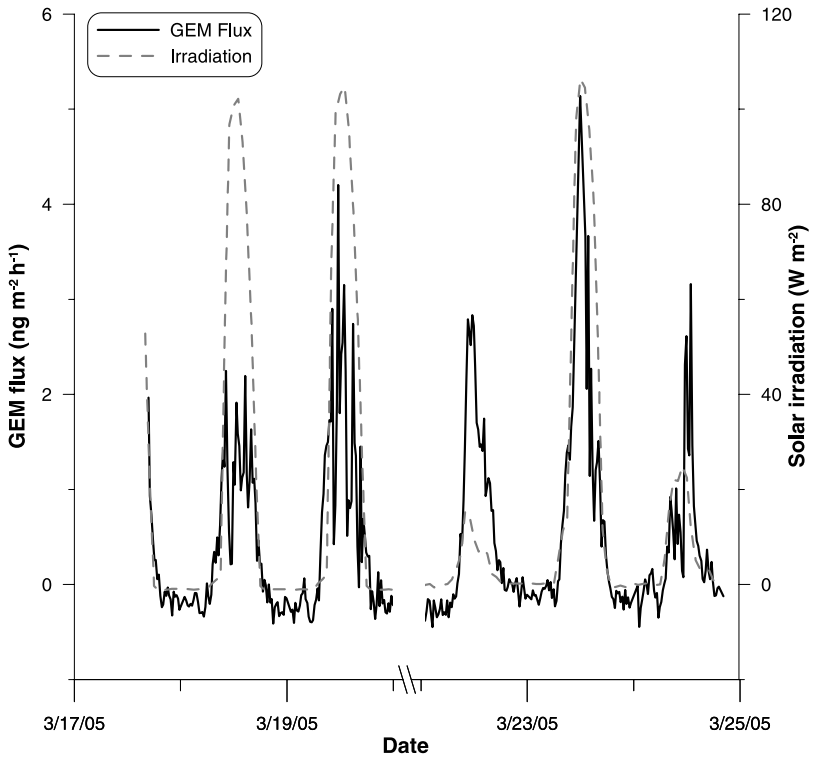

Figure 4. GEM fluxes (ng m^{-2} h^{-1}) from the snowpack to the atmosphere and solar irradiation (W m^{-2}) from March 17 to 24.

Table 2. GEM Fluxes (ng m^{-2} h^{-1}) From the Snowpack to the Atmosphere Measured During Daytime and Nighttime From 17 to 24 March

Time	Max Emission, ng m^{-2} h^{-1}	Integrated Emission, ng m^{-2} d^{-1}
18.03.2005[a]	1.4	7.84
19.03.2005[a]	3.08	12.09
20.03.2005[a]	2.28	10.22
23.03.2005[a]	3.34	12.2
24.03.2005[a]	1.63	5.64
Total[b]		49.99
Statistics[b]		
Mean	2.35	9.56
Std	0.86	2.83
P-value	5	5

[a]Day from 6:00 am to 9:00 pm.
[b]Values calculated from 5 days.

ration actually took place. We had no data from GEM in SIA at night as our probes could not be applied at night, but GEM concentrations at sunrise were always above atmospheric levels (see Figure 2).

3.6. Laboratory Flux Chamber Measurements

3.6.1. Irradiation Investigations

[20] In the laboratory, we first measured the evolution of GEM exchange fluxes with radiation intensity from 0 to 120 W m^{-2} [see *Balhmann et al.*, 2006 for details]. Such measurements were done using different filters. The snow was kept at −4°C. GEM fluxes exhibited linear relations with irradiation as reported in Table 3. At a constant radiation power of about 120 W m^{-2}, the maximum fluxes were 15.4 ng m^{-2} h^{-1}, 6.5 ng m^{-2} h^{-1} and 1.9 ng m^{-2} h^{-1} without a filter, with a 295 nm filter and with a 340 nm filter respectively. In the darkness and using the 295 nm filter, Table 3 reports a positive emission flux of about ∼0.4 ng m^{-2} h^{-1} which is not consistent with measurements carried out in the field. Using data presented on Table 3, we quantified the role of UVA, UVB and visible radiation in the snowpack. We identified the part of GEM emission due to three wavelength intervals corresponding to the different filters used: below 295 nm, from 295 to 340 nm, and above 340 nm. These results are presented in Figure 5 and show that both UVA (320–400 nm) and UVB (280–320 nm) wavelengths play an active role in photochemical processes in the snowpack. However, UVB light could be the most efficient for inducing GEM production.

3.6.2. Temperature Investigations

[21] Temperature data and consequently the influence of liquid water in the snowpack are reported in Figure 6, which shows the mercury emission flux as a function of time. Radiation phases during the experiment are indicated by shaded areas: we applied a radiation intensity of 120 W m^{-2} and a Pyrex filter to cut off wavelength below 295 nm throughout the experiment. At the beginning of the experiment, from 0 to 420 min, the temperature was kept at −4°C. After 425 min, the temperature of the chamber was set to +1.5°C allowing the snow to melt. As one can see in Figure 6, the flux exhibited several distinct patterns which are denominated by characters *a* to *d*.

[22] *Phase a.* During the first 300 min, the snow was kept in the dark at −4°C. The mean flux was 0.42 ± 0.05 ng m^{-2} h^{-1}. The chamber outlet mean concentration used for the determination of the GEM flux was 0.17 ± 0.02 ng m^{-3}.

[23] *Phase b*. During the next phase of the experiment we turned on the light and determined the photo induced flux over this sample at −4°C. The flux increased from 0.4 ng m^{-2} h^{-1} to about 8.2 ng m^{-2} h^{-1} within 20 min, which roughly corresponds to the turnover time of the chamber. After this rapid initial increase the flux decreased exponentially: the dashed line shows the extrapolated flux to the end of the experiment.

[24] *Phase c*. After 425 min the chamber temperature was set to +1.5°C allowing the snow to melt. With the beginning of the snowmelt, the flux increased from 5.9 ng m^{-2} h^{-1} to about 7.7 ng m^{-2} h^{-1} and then seemed to stabilize to a lower level of 6.8 ng m^{-2} h^{-1}.

[25] *Phase d.* When most of the snow had melted the emission of GEM from the snow suddenly decreased and stayed constant at about 2.0 ng m^{-2} h^{-1}.

4. Discussion

4.1. GEM in the Lower Atmosphere

[26] GEM atmospheric concentrations of 1.8 ± 0.4 ng m^{-3} measured at Col de Porte are close to the mean GEM concentration of about 1.82 ± 0.34 ng m^{-3} reported for the Wank station (47°31 N, 11°09 E, 1780 m a.s.l., Germany) in 1996 [*Slemr and Scheel*, 1998]. More recently, a subalpine site in Switzerland showed GEM concentrations of ∼1.6 ng m^{-3} during a summer measurement campaign [*Obrist et al.*, 2006]. No GEM gradient was observed between 10 and 200 cm above the snow surface at Col de Porte. This is in agreement with observations made in Barrow in the spring 2004. Indeed, *Aspmo* and coworkers observed a significant increase of GEM concentrations in a height of centimeters above the snow but they could not detect any significant concentration variations from 10 cm to 200 cm above the snowpack (*Aspmo*, personal communication). *Steffen et al.* [2002] reported homogenous GEM concentrations in the Arctic atmosphere within several meters above the snow surface during periods without any depletion event.

4.2. Mercury Balance in the Snowpack

[27] GEM in the SIA reached concentrations between 1.7 and 9 ng m^{-3}. As mentioned before, GEM data collected at 20 cm depth could be influenced by cosampling with ambient air, and by diffusion processes. A part of GEM formed in the snowpack close to the surface could diffuse immediately to the atmosphere. These considerations could explain that, after 10:00, the highest concentrations are not

Table 3. Linear Relations Between GEM Emission Fluxes and Radiation (R) Measured With a Cut Off of 340 nm, Cut Off of 295 nm and Without any Filter[a]

	$F_{GEM}(R)$	r^2	P-value
No Filter	0.107 × R + 0.564	0.99	11
Cut off 295 nm	0.048 × R + 0.348	0.98	10
Cut off 340 nm	0.010 × R + 0.744	0.88	11

[a]Radiation is in W m^{-2}, and GEM Flux in ng m^{-2} h^{-1}.

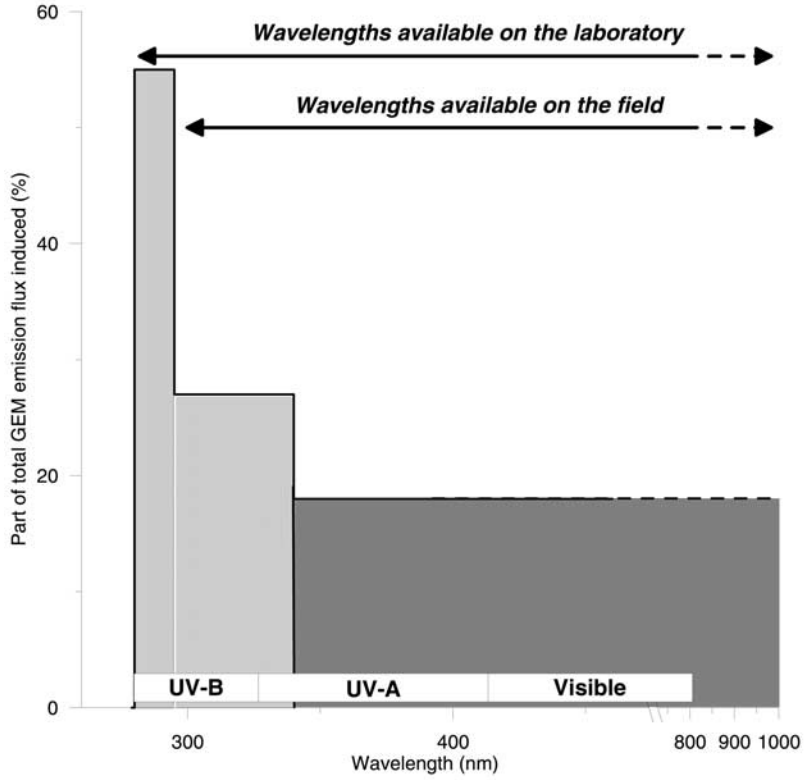

Figure 5. Schematic representation of the proportion of GEM emission induced by three wavelength intervals: below 295 nm, from 295 to 340 nm, and above 340 nm. Total GEM flux represents 100%. UVB (280–320 nm), UVA (320–400 nm) and visible (400–800 nm) intervals are represented. Arrows indicate the wavelengths available in the field and in the laboratory respectively.

measured anymore at 20 cm, but at 40 cm depth. GEM represented at Col de Porte approximately 0.1% of the mercury content in the snowpack. This value is comparable to the mercury balance in the Arctic snowpack estimated at Ny Ålesund (Svalbard) [*Ferrari et al.*, 2005] where GEM represented less than 1% of mercury. Total mercury exhibited a concentration range from 80 ± 08 ng l^{-1} to 160 ± 15 ng l^{-1} in the Col de Porte snowpack (see Table 1). This result is in good agreement with data reported by *Ferrari et al.* [2002] who measured Hg_T in different alpine snowpacks, including the Col de Porte snowpack. They obtained Hg_T concentrations as high as 130 ng l^{-1}. Such high concentrations of total mercury could be linked to anthropogenic influences and the proximity of a large urban area. Reactive mercury remained below the detection limit (0.2 ng l^{-1}) at all depths in the Col de Porte snowpack. *Ferrari et al.* [2002] measured Hg_R at the same location and also reported concentrations below their detection limit (which was about 0.8 ng l^{-1}). *Lalonde et al.* [2003] quantified Hg_R concentrations on a remote and temperate area in north-western Ontario (Canada) by gas-phase atomic fluorescence spectrometry with a detection limit of about 0.04 ng l^{-1}. They showed that 40% of Hg_R deposited during snow fall events were lost within 24 h due to reduction processes, with concentrations decreasing from ∼1.4 ± 0.5 ng l^{-1} to ∼0.8 ± 0.3 ng l^{-1}. Furthermore, measuring Hg_R in old snow layers, they obtained concentrations as low as 0.2 ± 0.1 ng l^{-1}. The concentrations we measured at Col de Porte are consistent with these data. Because the snow collected for Hg_R analysis was 10 days old, we assume that Hg_R previously deposited during wet events was completely lost. *Lalonde et al.* [2003] report that UVB-initiated Hg(II) reduction could lead to a net snow-to-air transfer of mercury. Our field and lab flux measurement support the hypothesis that Hg_R could be transformed after deposition. Production of GEM in the SIA was observed every day during our field work, and results obtained using our laboratory flux chamber suggest that UV radiation plays a key role in GEM emission from the snowpack (for more details see Section 4.4). Another option is that wet deposition could have been largely depleted in reactive mercury. Past studies on mercury speciation in clouds carried out at the site of Puy de Dome, 300 km from the area investigated, gave concentrations of about 10 to 50 ng l^{-1} for Hg_T and about 0.8 to 3.5 ng l^{-1} for Hg_R [*Gauchard et al.*, 2003]. Some recent research works also suggest that bacteria and microorganisms could interact with Hg_R in the snowpack [*Amato et al.*, 2007]. Possibly, the low measured Hg_R concentrations may be a combination of both minor wet deposition during snow fall episodes and destruction of reactive mercury complexes in the snowpack partially due to active photoreduction mechanisms that are discussed in Section 4.3.

4.3. The Alpine Snowpack, a Source of GEM

4.3.1. Irradiation and GEM Production

[28] Both destruction and production of GEM were observed in the SIA in polar areas [*Dommergue et al.*,

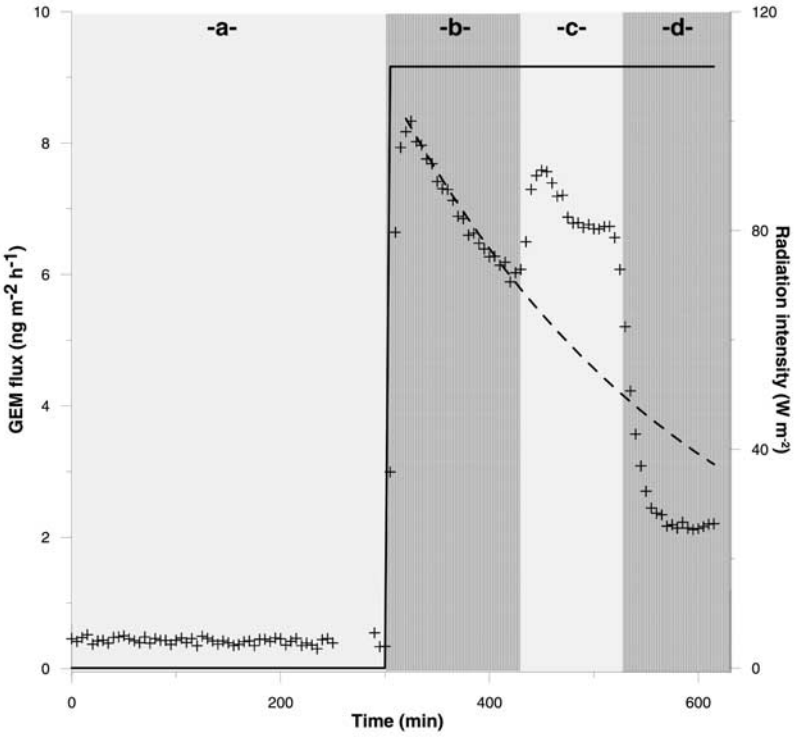

Figure 6. Variation of GEM flux (ng m^{-2} h^{-1}) with time measured in the laboratory flux chamber. Phase a reports dark flux at −4°C. During phase b, c and d, total irradiation was 120 W m^{-2} with wavelengths above 295 nm. Temperature in the chamber was kept at −4°C during phase b, and then increased to +1.5°C during phase c and d.

2003c; *Ferrari et al.*, 2004b]. In the arctic snowpack, GEM oxidation probably competes with Hg(II) reduction, and the SIA can exhibit GEM concentrations lower or higher than atmospheric levels. At Col de Porte, all the data collected during March 2005 from the surface to the bottom of the snowpack were above the atmospheric background (1.8 ng m^{-3}). Our results showed GEM production, but did not indicate the occurrence of GEM oxidation. GEM concentrations in the SIA and GEM emission from the snow surface at Col de Porte showed a diurnal pattern well correlated with solar irradiation as reported in Figures 3 and 5. These observations suggested that GEM production is driven by photolytic mechanisms. Previous studies have pointed out the role of irradiation in GEM production in the SIA [*Xiao et al.*, 1994; *Lalonde et al.*, 2002; *Dommergue et al.*, 2003c], and we observed at Col de Porte simultaneous increases of irradiation and GEM concentration at 20 cm depth (see Figure 2). A recent study showed that warmer, wetter and midlatitude snowpack are more transparent to UV radiation than dry and cold snowpacks from the high Arctic [*Fisher et al.*, 2005]. They also suggest that most of the photochemical reactions (85%) occur in the top 15–60 cm of the snowpack. Our alpine snowpack is warm around −2°C. We thus expect that photochemical reactions will occur from the surface to 40 cm depth. Deeper in the snowpack, as reported at 80 cm depth in Figure 2, a delay appears between the increase of GEM concentration and solar irradiation. Diffusion of GEM from the upper layer is therefore assumed to explain daily GEM variations in the bottom layers of the snowpack. The production of GEM at the surface of the snowpack could be the result of direct photodissociation of Hg(II) complexes, e.g., hydroxo or chlorocomplexes. *Ferrari et al.* [2002] showed that these complexes represent the predominant mercury species in the alpine snowpack. These reduction mechanisms were observed in water solutions [*Xiao et al.*, 1994] and suggested to occur in snow [*Lalonde et al.*, 2002, 2003]. However, GEM could also be produced by the reduction of Hg(II) complexes by photochemically produced compounds: hydroperoxyl radical (HO_2) was proposed as a potential reductant of Hg(II) in the snow [*Lin and Pehkonen*, 1999]. However, this hypothesis has to be considered carefully, since a recent study based on thermodynamical considerations showed that reduction of Hg(II) to GEM by HO_2 radicals should be of minor importance [*Gardfeldt and Jonsson*, 2003]. Moreover, even if we were not able to measure GEM in the SIA during the night, we noticed higher concentrations than atmospheric ones in the whole snowpack and especially in the surface layers (see Figure 2 with 2.6 ng m^{-3} at 20 cm depth and 3.4 ng m^{-3} at 40 cm depth before 6:30 am) at sunrise. It suggests that the reduction of Hg(II) could also be possible in the dark. This production of GEM in the dark has also been reported in snow samples collected in a midlatitude snowpack [*Lalonde et al.*, 2003] and inside an arctic snowpack [*Ferrari et al.*, 2004b].

4.3.2. Influence of Liquid Water in the Snowpack

[29] An increase of the snow temperature can affect GEM production in the alpine snowpack. We observed a significant increase of GEM concentrations in the snowpack

when the snow was melting as displayed in Figure 3. The link between snow temperature and GEM production has been reported for an arctic snowpack in Ny Ålesund, Svalbard [*Ferrari et al.*, 2005]. *Dommergue et al.* [2003b] measured peak GEM emission fluxes around 25 ng m^{-2} h^{-1} at Kuujjuarapik (Quebec, Canada) during the first day of snowmelt. *Lalonde et al.* [2003] observed significant photoreduction of Hg(II) complexes during snowmelt at temperate latitudes. Liquid water in the snowpack could enhance GEM production. The increase of snow temperature leads to an increase of the thickness of the water films around snow grains. This liquid layer is an active chemical reactor around snow grains [*Takenaka et al.*, 1992]. *Bales et al.* [1990] showed that ionic species accumulated during snow precipitation and finally concentrated in snow grains could be released in the earliest fraction of meltwater. This ionic pulse could also affect Hg(II) complexes. Reduction reactions could take place in the aqueous phase with enhanced reaction rates [*Xiao et al.*, 1994]. They showed that mercury complexes are efficiently photodissociated in aqueous solutions. Such photodissociation reactions may occur in snow [*Lalonde et al.*, 2002, 2003] and could be enhanced during snowmelt by the presence of liquid water in the snowpack.

4.3.3. GEM Fluxes From the Snowpack to the Atmosphere

[30] GEM emission fluxes measured at Col de Porte are quite close to fluxes reported for arctic and sub-arctic snowpacks if we do not consider large emissions measured immediately after AMDEs [*Dommergue et al.*, 2003c; *Schroeder et al.*, 2003; *Ferrari et al.*, 2005; *Brooks et al.*, 2006]. GEM fluxes from the snowpack to the atmosphere exhibited a diel pattern correlated with solar radiation for the whole period of the study (see Figure 4). These results confirm that GEM production in the snowpack is mainly due to photochemical mechanisms. Some measurements of GEM concentrations in the SIA before sunrise suggested dark production of GEM at night. Such dark production did not induce any detectable emission flux from the snow surface.

4.4. Modeling of Field Observations Using Laboratory Measurements

[31] Temperature in the snowpack and solar radiation were identified in the field to be the main environmental parameters driving GEM production in the SIA. Laboratory investigations with a flux chamber confirmed these observations, and enable a better simulation of GEM production processes.

4.4.1. Effect of Irradiation

[32] As reported in Table 3, there is a linear relationship between the GEM flux and the radiation intensity over different spectral ranges. These results support the hypothesis that the reemission of GEM from snowpacks is mostly driven by solar radiation. We calculated GEM emission ratios from our irradiation experiments with UVA, UVB and visible light. All ratios were independent of the radiation intensity. It is therefore concluded that UVA (320–400 nm) could induce GEM production, whereas UVB (280–320 nm) is the most efficient spectral band for GEM production. When the snow was exposed to light with unfiltered light (providing some UV wavelengths which are not available at the Earth's surface), the fluxes measured were twice as high as those measured with a spectrum available at the Earth's surface. However, one must notice that the use of a filter reduced the intensity of irradiation of about 10% over the entire spectrum. As we used GEM-free air at the inlet of the chamber, we were not representative of the atmospheric GEM background of ~1.8 ng m^{-3}. We artificially created high gradients between the SIA and the air above the snow surface in the laboratory. The GEM concentration at which no exchange occurs between the snow surface and the chamber is termed the compensation point [*Hanson et al.*, 1995]. This compensation point increased with radiation considering snow samples from Col de Porte. We obtained surprisingly a good agreement between field and laboratory flux data for high radiation values. For radiation of ~80 W m^{-2}, laboratory measurements gave a flux of ~4 ng m^{-2} h^{-1} using a cut-off of 295 nm (this filter enable to reproduce natural light radiation under clear sky conditions). This value is close to the fluxes measured in the field at midday (see Figure 4). However, considering low radiation values, the light induced fluxes measured in the laboratory were significantly higher than these obtained in the field. We assumed that the compensation point was high compared to 1.8 ng m^{-3} at ~80 W m^{-2}, but between 0 and 1.8 ng m^{-3} in dark conditions. Finally, the GEM flux observed in the darkness had no relevance to natural conditions. The laboratory measurements did not allow us to explain GEM chemistry in the Col de Porte snowpack at night.

4.4.2. Kinetic Considerations

[33] With constant radiation and temperature (phase b, Figure 6), the GEM flux decreased exponentially indicating a pseudo first order reaction. Without any filter the decay of the flux was given by:

$$F = 15.4 \times \exp(-0.185 \times t), \left(r^2 = 0.97, n = 41\right), \text{ in ng } m^{-2}h^{-1}$$

[34] The dashed line on Figure 6 indicates the expected decay of the flux with a cut off of 295 nm. This decay could be described by the following equation:

$$y = 6.5 \times \exp(-0.238 \times t), \left(r^2 = 0.98, n = 16\right)$$

[35] These data imply that 95% of the Hg(II) available for photoreduction was reduced within 16.2 h (filter 295 nm) and 12.6 h (no filter) respectively. It is noteworthy that the flux decreased with different time constants for the different spectral ranges. With a cut off of 295 nm, the kinetic constant was ~0.238 h^{-1}. The corresponding lifetime was ~4 h. This value could be compared to previous studies. It was lower than the photolysis rate constant of $Hg(OH)_2$ in aqueous phase given by *Xiao et al.* [1994], who found a value of ~0.432 h^{-1}. For freshwaters exposed to light, *Zhang and Lindberg* [2001] determined rate constants between ~0.1 and 0.3 h^{-1} for GEM production.

[36] As the penetration of UVB radiation into snowpacks is limited to the top layers of the snow [*Fisher et al.*, 2005], we also assessed the effect of mechanical disturbance of the top snow stratification on the light induced emission of mercury. A snow sample was exposed to light (cut off of 295 nm) for 3 h. Then the radiation was stopped and the

surface of the snow (~1 cm) was mechanically disturbed with a stainless steel spatula and afterward the radiation was continued for one additional hour. At the beginning of the experiment, we observed a flux of 6.1 ng m^{-2} h^{-1} which decreased to 3.5 ng m^{-2} h^{-1} after 3 h and recovered to 4.9 ng m^{-2} h^{-1}. Even if the flux did not completely recover, this data clearly show that mechanical or physical disturbance at the snow surface, e.g., due to melting, may recharge the mercury pool at the snow surface available for photoreduction.

4.4.3. The Role of Temperature and Liquid Water

[37] Phase c in Figure 6 shows the influence of the temperature in the snowpack on GEM production. When liquid water appeared in the snowpack, GEM emission flux rapidly increased to 7.7 ng.m^{-2}.h^{-1}, and then stabilized at ~7 ng m^{-2} h^{-1}. As discussed before, we assume that liquid layers around snow grains could act as a chemical reactor, concentrating ionic species. A large exchange area between water and the SIA, and higher kinetic rates in the aqueous phase could explain the higher fluxes. This hypothesis is further supported by the rapid decrease reported in phase d. When the snow has melted almost entirely, the exchange surface between water and air suddenly decreased, and all the ionic species, which were previously concentrated in a thin water film, were now diluted in a large volume of water. These preliminary results show that the fate of mercury during snowmelt could be a rapid reduction of Hg_R complexes in the snowpack followed by an emission of GEM to the atmosphere. However, Hg_R complexes could also be transferred to the meltwater where exchange with the atmosphere is much more limited. Hence mercury could become available for accumulation in ecosystems.

4.5. Fate of Mercury Species During Snowmelt

[38] *Dommergue et al.* [2003b] reported total mercury concentrations of about ~22.5 ng l^{-1} in surface snow and ~10.0 ng l^{-1} in meltwater samples at Kuujjuarapik (Quebec, Canada). At Col de Porte we measured concentrations almost one order of magnitude higher, with ~160 ng l^{-1} in surface snow and 79 ± 1, 63 ± 3 and 74 ± 2 ng l^{-1} in three meltwater samples. We obtained the same ratio between surface snow and meltwater concentrations at Col de Porte than at Kuujjuarapik, Quebec [2003c]. These preliminary results are of prime importance as they suggest that an important release of mercury could occur at springtime during snowmelt. Mercury levels in alpine meltwater are considerably higher than concentrations of ~1–7 ng l^{-1} reported for non-polluted river water [*Poissant*, 2002]. Further studies addressing the vulnerability and contamination of alpine ecosystems are needed, even if this release of mercury could occur in a limited period of the year.

5. Conclusion

[39] The present study reported GEM production and the exchange fluxes between the snowpack and the atmosphere in an alpine snowpack during snowmelt in spring 2005. Concentration of Hg_R was below detection limit and GEM in interstitial air represented less than 1% of the mercury in snowpack layers. The exchanges of GEM between the snowpack and the atmosphere were mostly driven by Hg(II) reduction during daytime, with mean integrated emissions from 5.64 to 12.20 ng m^{-2} d^{-1}. We demonstrated that liquid water in the snowpack enhanced GEM production. Irradiation and snow temperature played a key role in internal photoproduction of GEM, most likely by increasing the liquid layers at the surface of snow grains. These results were validated by laboratory flux chamber measurements: we were able to quantify the role of irradiation on GEM production.

[40] Rapid depletion of GEM has been observed in arctic snowpacks [*Dommergue et al.*, 2003c; *Ferrari et al.*, 2004b]. Halogen compounds such as bromine radicals were proposed to explain the involved oxidation processes [*Ariya et al.*, 2004; *Goodsite and Plane*, 2004]. Our results in the French Alps are in good agreement with this hypothesis: the alpine atmosphere, and thus the alpine snowpack, are poor in halogen compounds and no important GEM depletion could be observed neither in the atmosphere nor in the SIA.

[41] Preliminary studies of meltwater indicated higher levels of Hg as compared to non-polluted waters. Further studies are needed to better assess the fate of mercury during snowmelt in temperate areas as it could negatively affect drinking water quality.

[42] **Acknowledgments.** This research was funded by A.D.E.M.E. (Agence de l'Environnement et de la Maitrise de l'Energie, Programs 0162020 and 0462C0108) and the French PNCA program "Echanges Neige Polaire". We would like to thank the French Ministry of Research for its financial support of young scientists (so called A.C.I. JC 3012). Claude Boutron and Christophe Ferrari thank the Institut Universitaire de France (I.U.F.) for its financial help for this study. We thank Meteo-France and CEN staff for giving us the opportunity to work at the Col de Porte station, and for providing us meteorological data. We thank Florent Dominé for measuring the physical properties of the snowpack, and for his helpful comments concerning the snow characteristics.

References

Albert, M. R., and E. F. Shultz (2002), Snow and firn properties and air-snow transport processes at Summit, Greenland, *Atmos. Environ.*, *36*(15–16), 2789–2797.

Albert, M. R., A. M. Grannas, J. Bottenheim, P. B. Shepson, and F. E. Perron Jr. (2002), Processes and properties of snow-air transfer in the high arctic with application to interstitial ozone at Alert, Canada, *Atmos. Environ.*, *36*, 2779–2787.

Amato, P., R. Hennebelle, O. Magand, M. Sancelme, A. M. Delort, C. Barbante, C. Boutron, and C. Ferrari (2007), Bacterial characterization of the snowcover at Spitzberg, Svalbard, *FEMS Microbiol. Ecol.*, *59*(2), 242–254.

Ariya, P. A., et al. (2004), The Artic, a sink for mercury, *Tellus*, *56B*, 397–403.

Bales, R. C., R. Sommerfel, and D. Kebler (1990), Ionic tracer movement through a Wyoming snowpack, *Atmos. Environ.*, *24*, 2749–2758.

Bales, R. C., M. V. Losleben, J. R. McConnell, K. Fuhrer, and A. Neftet (1995), H_2O_2 in snow, air and open pore space in firn at Summit, Greenland, *Geophys. Res. Lett.*, *22*(10), 1261–1264.

Balhmann, E., R. Ebinghaus, and W. Ruck (2006), Development and application of a laboratory flux measurement system (LFMS) for the investigation of the kinetics of mercury emissions from soils, *J. Environ. Monit.*, *81*, 114–125.

Blais, J. M., S. Charpentié, F. Pick, L. E. Kimpe, A. St Amand, and C. Regnault-Roger (2005), Mercury, polybrominated diphenyl ether, organochlorine pesticide, and polychlorinated biphenyl concentrations in fish from lakes along an elevation transect in the French Pyrénées, *Ecotoxicol. Environ. Saf.*, *63*(1), 91–99.

Boutron, C. F. (1990), A clean laboratory for ultra-low concentration heavy metal analysis, *J. Anal. Chem.*, *337*, 482–491.

Brooks, S., A. Saiz-Lopez, H. Skov, S. Lindberg, J. M. C. Plane, and M. Goodsite (2006), The mass balance of mercury in the springtime arctic environment, *Geophys. Res. Lett.*, *33*, L13812, doi:10.1029/2005GL025525.

Dommergue, A., C. P. Ferrari, F. Planchon, and C. F. Boutron (2002), Influence of anthropogenic sources on total gaseous mercury variability in Grenoble suburban air (France), *Sci. Total Environ.*, *297*, 203–213.

Dommergue, A., C. P. Ferrari, and C. F. Boutron (2003a), First investigation of an original device dedicated to the determination of gaseous mercury in interstitial air in snow, *Anal. Bioanal. Chem.*, *375*, 106–111.

Dommergue, A., C. P. Ferrari, P.-A. Gauchard, C. F. Boutron, L. Poissant, M. Pilote, F. Adams, and P. Jitaru (2003b), The fate of mercury species in a sub-arctic snowpack during the snowmelt, *Geophys. Res. Lett.*, *30*(12), 1621, doi:10.1029/2003GL017308.

Dommergue, A., C. P. Ferrari, L. Poissant, P.-A. Gauchard, and C. F. Boutron (2003c), Diurnal cycles of gaseous mercury within the snowpack at Kuujjuarapik/Whapmagoostui, Québec, Canada, *Environ. Sci. Technol.*, *37*(15), 3289–3297.

Dommergue, A., E. Balhmann, R. Ebinghaus, C. Ferrari, and C. Boutron (2007), Laboratory simulation of Hg° emissions from a snowpack, *Anal. Bioanal. Chem.*, doi:10.1007/s00216-007-1186-2.

Ebinghaus, R., H. H. Kock, C. Temme, J. W. Einax, A. G. Löwe, A. Richter, J. P. Burrows, and W. H. Schroeder (2002), Antarctic springtime depletion of atmospheric mercury, *Environ. Sci. Technol.*, *36*(6), 1238–1244.

Engle, M. A., M. S. Gustin, and H. Zhang (2001), Quantifying natural source mercury emissions from Ivanhoe Mining Destrict, north-central Nevada, USA, *Atmos. Environ.*, *35*, 3987–3997.

EPA (1998), Method 7473: Mercury in solids and solutions by thermal decomposition, amalgamation, and atomic absorption spectrophotometry, pp. 36.

Ferrari, C. P., A. L. Moreau, and C. F. Boutron (2000), Clean conditions for the determination of ultra-low levels of mercury in ice and snow samples, *J. Anal. Chem.*, *366*, 433–437.

Ferrari, C. P., A. Dommergue, A. Veysseyre, F. A. M. Planchon, and C. F. Boutron (2002), Mercury speciation in the French seasonal snow cover, *Sci. Total Environ.*, *287*(1–2), 61–69.

Ferrari, C. P., A. Dommergue, and C. F. Boutron (2004a), Profiles of Mercury in the snow pack at Station Nord, Greenland shortly after polar sunrise, *Geophys. Res. Lett.*, *31*, L03401, doi:10.1029/2003GL018961.

Ferrari, C. P., A. Dommergue, H. Skov, M. Goodsite, and C. F. Boutron (2004b), Nighttime production of elemental gaseous mercury in interstitial air of snow at Station Nord, Greenland, *Atmos. Environ.*, *38*, 2727–2735.

Ferrari, C., et al. (2005), Snow-to-air exchanges of mercury in an Arctic seasonal snow pack in Ny-Alesund, Svalbard, *Atmos. Environ.*, *39*, 7633–7645.

Fisher, F. N., M. D. King, and J. Lee-Taylor (2005), Extinction of UV-visible radiation in wet midlatitude (maritime) snow: Implications for increased NOx emission, *J. Geophys. Res.*, *110*, D21301, doi:10.1029/2005JD005963.

Fritsche, J., D. Obrist, and C. Alewell (2006), Evidence of microbial control of Hg^0 emissions from uncontaminated terrestrial soils, *submitted to J. Plant Nutr. Soil Sci.*

Gardfeldt, K., and M. Jonsson (2003), Is bimolecular reduction of Hg(II) complexes possible in aqueous systems of environmental importance, *J. Phys. Chem.*, *107*, 4478–4482.

Gauchard, P.-A., A. Dommergue, C. P. Ferrari, L. Poissant, and C. Boutron (2003), Mercury speciation into tropospheric clouds, in *VIIth International Conference on Mercury as a Global Pollutant*, pp. 1577, RMZ-Materials and Geoenvironment, Ljubljana, Slovenia.

Goodsite, M. E., and J. M. C. Plane (2004), A Theoretical study of the oxidation of Hg° to $HgBr_2$ in the Troposphere, *Environ. Sci. Technol.*, *38*, 1772–1776.

Hanson, P. J., S. Lindberg, T. Tabberer, J. Owens, and K.-H. Kim (1995), Foliar exchange of mercury vapor: Evidence for a compensation point, *Water, Air, Soil Pollut.*, *80*, 373–382.

Honrath, R. E., Y. Lu, M. C. Peterson, J. E. Dibb, M. A. Arsenault, N. J. Cullen, and K. Steffen (2002), Vertical fuxes of NO_x; HONO, and HNO_3 above the snowpack at Summit, Greenland, *Atmos. Environ.*, *36*, 2629–2640.

Lalonde, J. D., A. J. Poulain, and M. Amyot (2002), The role of mercury redox reactions in snow on snow-to-air mercury transfer, *Environ. Sci. Technol.*, *36*(2), 174–178.

Lalonde, J. D., M. Amyot, M.-R. Doyon, and J.-C. Auclair (2003), Photo-induced Hg(II) reduction in snow from the remote and temperate Experimental Lake Area (Ontario, Canada), *J. Geophys. Res.*, *108*(D6), 4200, doi:10.1029/2001JD001534.

Lamborg, C. H., W. F. Fitzgerald, J. O'Donnell, and T. Torgersen (2002), A nonsteady-state compartmental model of global-scale mercury biogeochemistry with interhemispheric atmospheric gradients, *Geochim. Cosmochim. Acta*, *66*, 1105–1118.

Lin, C.-J., and S. O. Pehkonen (1999), The chemistry of atmospheric mercury: A review, *Atmos. Environ.*, *33*, 2067–2079.

Lindberg, S. E., S. Brooks, C.-J. Lin, K. J. Scott, M. S. Landis, R. K. Stevens, M. Goodsite, and A. Richter (2002), Dynamic oxidation of gaseous mercury in the Arctic troposphere at polar sunrise, *Environ. Sci. Technol.*, *36*(6), 1245–1256.

Lindqvist, O., and H. Rodhe (1985), Atmospheric mercury - A review, *Tellus*, *37B*, 136–159.

Obrist, D., M. S. Gustin, J. A. Arnone, D. W. Johnson, D. E. Schorran, and P. S. J. Verburg (2005), Measurements of gaseous elemental mercury fluxes over intact tallgrass prairie monoliths during one full year, *Atmos. Environ.*, *39*, 957–965.

Obrist, D., F. Conen, R. Vogt, R. Siegwolf, and C. Alewell (2006), Estimation of Hg° exchange between ecosystems and the atmosphere using 222Rn and Hg° concentration changes in the stable nocturnal boundary layer, *Atmos. Environ.*, *40*, 856–866.

Pacyna, J. M., and G. J. Keeler (1995), Sources of mercury in the Arctic, *Water, Air, Soil Pollut.*, *80*, 621–632.

Pacyna, E. G., J. M. Pacyna, and N. Pirrone (2001), European emissions of atmospheric mercury from anthropogenic sources in 1995, *Atmos. Environ.*, *35*(17), 2987–2996.

Petersen, G., R. Bloxam, S. Wong, J. Munthe, O. Krüger, S. R. Schmolke, and A. Vinod Kumar (2001), A comprehensive Eulerian modelling framework for airborne mercury species: model development and applications in Europe, *Atmos. Environ.*, *35*(17), 3063–3074.

Poissant, L. (2002), Mercury surface-atmosphere gas exchange in Lake Ontario/St. Lawrence river ecosystem, *Revue des Sciences de l'Eau*, *15*, 229–239.

Pyle, D. M., and T. A. Mather (2003), The importance of volcanic emissions for the global atmospheric mercury cycle, *Atmos. Environ.*, *37*, 5115–5124.

Roos-Barraclough, F., N. Givelet, A. Martinez-Cortizas, M. E. Goodsite, H. Biester, and W. Shotyk (2002), An analytical protocol for the determination of total mercury concentrations in solid peat samples, *Sci. Total Environ.*, *292*, 129–139.

Schroeder, W. H., and J. Munthe (1998), Atmospheric mercury - An overview, *Atmos. Environ.*, *32*(5), 809–822.

Schroeder, W. H., G. Keeler, H. Kock, P. Roussel, D. Schneeberger, and F. Schaedlich (1995), International field intercomparison of atmospheric mercury measurement methods, *Water, Air, Soil Pollut.*, *80*, 611–620.

Schroeder, W. H., A. Steffen, K. Scott, T. Bender, E. Prestbo, R. Ebinghaus, J. Y. Lu, and S. E. Lindberg (2003), Summary report: First international Arctic atmospheric mercury research workshop, *Atmos. Environ.*, *37*(18), 2551–2555.

Slemr, F., and H. E. Scheel (1998), Trends in atmospheric mercury concentrations at the summit of the Wank mountain, southern Germany, *Atmos. Environ.*, *32*(5), 845–853.

Slemr, F., E. G. Brunke, R. Ebinghaus, C. Temme, J. Munthe, I. Wangberg, B. Schroeder, A. Steffen, and T. Berg (2003), Worldwide trend of atmospheric mercury since 1977, *Geophys. Res. Lett.*, *30*(10), 1516, doi:10.1029/2003GL016954.

Steffen, A., W. H. Schroeder, J. Bottenheim, J. Narayana, and J. D. Fuentes (2002), Atmospheric mercury concentrations: Measurements and profiles near snow and ice surfaces in the Canadian Arctic during Alert 2000, *Atmos. Environ.*, *36*(15–16), 2653–2661.

Sumner, A. L., and P. B. Shepson (1999), Snowpack production of formaldehyde and its effect on the Arctic troposphere, *Nature*, *398*, 230–233.

Takenaka, N., A. Ueda, and Y. Maeda (1992), Acceleration of the rate of nitrite oxidation by freezing in aqueous solution, *Nature*, *358*, 736–738.

Xiao, Z. F., J. Munthe, D. Strömberg, and O. Lindqvist (1994), Photocemical behavior of inorganic mercury compounds in aqueous solution, in *Mercury as a Global Pollutant - Integration and Synthesis*, edited by C. J. Watras and J. W. Huckabee, pp. 581–592, Lewis Publishers, Boca Raton.

Zhang, H., and S. E. Lindberg (2001), Sunlight and Iron(III)-induced photochemical production of dissolved gaseous mercury in freshwater, *Environ. Sci. Technol.*, *35*, 928–935.

E. Bahlmann, C. Boutron, A. Dommergue, X. Faïn, C. P. Ferrari, and S. Grangeon, Laboratoire de Glaciologie et Géophysique de l'Environnement (UMR 5183 CNRS/Université Joseph Fourier), 54, rue Molière, B.P. 96, 38402 St Martin d'Heres cedex, France. (fain@lgge.obs.ujf-grenoble.fr)

C. Barbante, W. Cairns, and P. Cescon, Environmental Sciences Department, University of Venice, Calle Larga S. Marta, 2137, I-30123 Venice, Italy.

R. Ebinghaus, Institute for Coastal Research, GKSS Research Centre, Max-Planck-Street 1, D-21502 Geesthacht, Germany.

J. Fritsche, Institute of Environmental Geosciences, University of Basel, Bernoullistrasse 30, 4056 Basel, Switzerland.

D. Obrist, Desert Research Institute, Division of Atmospheric Sciences, 2215 Raggio Parkway, Reno, NV 89512, USA.